plume precluded the simultaneous unambiguous measurement of both the reflected and the transmitted signal, which would have permitted the collision frequency (ν_c) to be determined in addition to the electron density. Estimates of ν_c/ω for the plume used in these preliminary tests indicated a value in the range of 0.005 to 0.015. For a given value of the reflected signal, the calculated electron density is relatively insensitive to the precise value of ν_c/ω when this quantity is small, as it is in the case in question. This uncertainty is indicated by the error brackets shown on the data points.

The arm is well suited for higher microwave probing frequencies where the "saturation core" will be reduced and the spatial resolution increased because of the shorter wavelengths involved. In addition, the restrictions on plasma size will be lessened since the characteristic dimensions for permissible gradients will also be reduced. The probe can also be used to take time-resolved data at selected positions within the plume where the observation time is small in comparison with the dwell time in the plume.

References

[1] Jahn, R. G., "Microwave probing of ionized-gas flows," Phys. Fluids **5**, 678–686 (1962).

[2] Kritz, A. H.," Microwave interactions with inhomogeneous partially ionized plasmas," Western States Section/Combustion Institute Paper 62-20, Space Science Lab., General Dynamics/Astronautics, San Diego, Calif. (no date).

Energy Partition in the Current Layers in Plasma

JAN ROSCISZEWSKI*
General Dynamics/Astronautics, San Diego, Calif.

1. Introduction

MANY plasma propulsion systems are based on the principle that the moving current layer sweeps out the gas.[1] This principle seems to lead to devices of limited efficiency as the internal energy becomes a significant fraction of the total energy.

The stationary rarefaction ("deflagration") type of discharge layer provides a decrease in internal energy across the layer, and therefore should lead to much more efficient devices. It seems that the deflagration type of current layer occurs in the Giannini Corporation device.[2]

In the present paper, these two types of discharge layers are discussed from the gasdynamic point of view rather than propulsion application. The quantitative analysis of the discharge layer requires solution of the structure of such a layer, a difficult problem because of the multifluid nature of the discharge layer. However, quantitative information can be obtained by discussing only conservation relations across a layer.

2. Conservation Relations across the Current Layer

Conservation relations across the discharge layer in the form presented below can be derived from the differential equations for one-dimensional nonsteady multifluid model obtained by taking the moments of Boltzmann's equation.

Subsequently these equations have been transformed to the system of coordinates moving with the velocity of the back of the current layer ($\xi = \int V_p dt - x$, $\tau = t$. Integrating these differential equations across the current layer between two sections, 1 and 2 (Fig. 1) where there are no gradients of flow parameters, and applying the rule of differentiating the integral with variable boundary

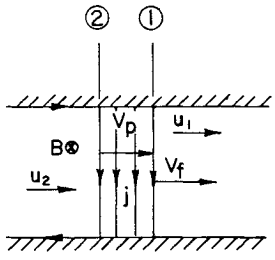

Fig. 1 Current layer geometry.

$$\int_0^{\delta_1} \frac{\partial F}{\partial \tau}\, d\xi = \frac{d}{d\tau}\int_0^{\delta_1(\tau)} F d\xi - F_1 \frac{d\delta_1}{d\tau}$$

with $d\delta/d\tau = V_f - V_p$, one obtains the conservation relations in the following form†:

Conservation of Mass (Fig. 1)

$$\rho_1(V_f - u_1) - \rho_2(V_p - u_2) = \frac{d}{d\tau}\int_0^{\delta_1} \rho d\xi \equiv \frac{dM}{d\tau} \qquad (1)$$

where

V_f = the velocity of the front of the discharge layer
V_p = the velocity of the back of the discharge layer
ρ = nm = the mass density
δ_1 = the thickness of the discharge layer

and u_1 and u_2 are the gas velocities (in laboratory frame) ahead and behind the discharge layer, respectively.

The left-hand side of Eq. (1) represents the difference between the mass flux entering and leaving the current layer; the right-hand side represents mass accumulated in the current layer.

Conservation of Momentum:

$$\rho_1(V_f - u_1) - p_1 - \frac{B_1^2}{2\mu} - \rho_2 \times (V_p - u_2)u_2 + p_2 + \frac{B_2^2}{2\mu} = \frac{d}{d\tau}\int u dM \qquad (2)$$

The energy equation can be written as follows[4]:

$$(V_p - u_2)\left[\rho_2 \frac{u_2^2}{2} + \frac{kn_2T_2}{\gamma - 1}\right] - (V_f - u_1)\left[\rho_1 \frac{u_1^2}{2} + \frac{kn_1T_1}{\gamma - 1}\right] - u_2 kn_2T_2 + u_1 kn_1T_1 = \frac{d}{d\tau}\int_0^{\delta}\left(\rho \frac{u^2}{2} + \frac{knT}{\gamma - 1} + \frac{B^2}{2\mu}\right) d\xi - \frac{dq_{\text{rad}}}{d\tau} + E_2'B_2 + u_2\frac{B_2^2}{2\mu} - E_1'B_1 - u_1\frac{B_1^2}{2\mu} \qquad (3)$$

where q_{rad} is the energy loss by radiation, E, E' denotes electric field in laboratory frame and moving frame, respectively.

Equations (1–3) become the shock-wave matching conditions when time derivatives of integrals on the right-hand sides disappear (no mass accumulation effects).

3. Application to the Magnetic Piston Problem

Assuming

$$B_1 = 0,\ T_1 \cong 0 \qquad E_2' = -(V_p - u_2)B_2 \qquad (4)$$

$$\frac{d}{d\tau}\left[\int_M e_{\text{int}}\, dM + q_{\text{rad}}\right] \equiv \frac{dW}{d\tau} = (2u_2 - V_p)\frac{d}{d\tau}\int_M u dM - \frac{d}{d\tau}\int_M \frac{u^2}{2} dM - (V_p - u_2)\left[\rho_2 \frac{u_2^2}{2} - \frac{kn_2T_2}{\gamma - 1}\right] - (V_f - u_1) \times \rho_1\left[\frac{u_1^2}{2} - u_1u_2 + \frac{kn_1T_1}{(\gamma - 1)\rho_1}\right] \qquad (5)$$

where $e_{\text{int}} = knT/(\gamma - 1) + (B^2/2\mu)$.

Received August 25, 1964, revision received October 5, 1964. The author appreciates many fruitful discussions with D. E. T. F. Ashby. This work was supported by Air Force Office of Scientific Research Contract AF 49(638)-1357.

* Consultant, Space Science Laboratory. Member AIAA.

† Full derivation of these equations is given in Ref. 3.

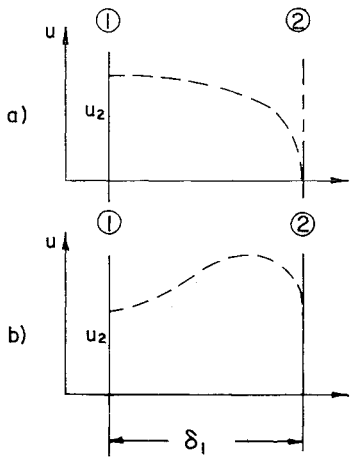

Fig. 2 Possible velocity distributions in the current layer.

To make use of expression (5), one has to know the velocity distribution across the discharge layer. However, one can make a qualitative analysis assuming different velocity distributions.

The simplest case is the one with constant velocity in the discharge layer $u = u_2(t)$

$$\frac{dW}{d\tau} = \left(\frac{3}{2}u_2 - V_p\right)\frac{d}{d\tau}\int\frac{u_2^2}{2}\,dM - (V_p - u_2)\times$$
$$\left[\rho_2\frac{u_2^2}{2} - \frac{kn_2T_2}{\gamma - 1}\right] - (V_f - u_1)\left[\rho_1\frac{u_1^2}{2} - \frac{kn_2T_2}{\gamma - 1}\right] \quad (6)$$

From this expression, it follows that any leakage across the magnetic piston ($u_2 < V_p$) decreases the internal energy.

With no leakage ($u_2 = V_p$)

$$W = \int(u_2^2/2)dM \quad (7)$$

In other words, the radiated plus internal energy is equal to the mean kinetic energy.

For the case of the velocity distribution presented in Fig. 2a steepening up wave,

$$W > \int(U_m^2/2)dM \quad (8)$$

where

$$u_m = (1/M)\int u dM$$

is the mean velocity in the layer. Therefore, the mean internal energy plus radiation energy is greater than the mean kinetic energy. If, however, one has the velocity distribution plotted in Fig. 2b,

$$W < \int(u_m^2/2)dM$$

Such a distribution of velocity would correspond to the case of the expanding current layer, resulting in better efficiency.

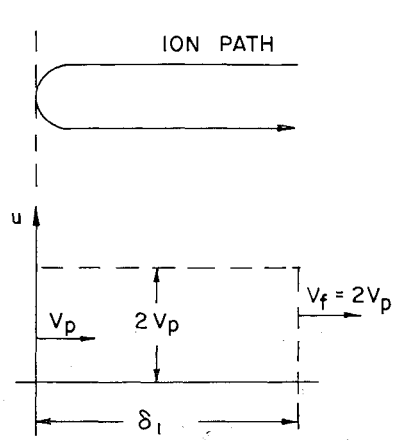

Fig. 3 Rosenbluth current sheet.

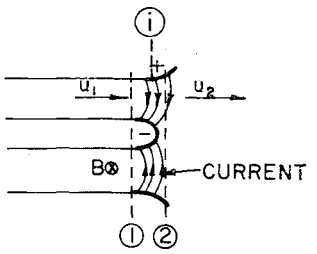

Fig. 4 Stationary current sheet.

4. Rosenbluth Sheet Model

In the Rosenbluth sheet model, particles are reflected from the sheet and move forward with a velocity equal to twice the sheet speed $V_f = 2V_p$ (Fig. 3). At the back edge of the sheet section 2, $u_2 = V_f$. However, in the volume between sections 1 and 2, only $\frac{1}{2}$ of mass is moving. Substituting $u = 2V_f$, one obtains from expression (5)

$$(dW/d\tau) = 0$$

Therefore, there is no energy loss, and the efficiency of such a device would be very good. However, the Rosenbluth sheet model has not been observed experimentally.

5. Deflagration Type of Discharge Layer

On the other hand, the accelerator process in the arcjet (operating at low density and high current (Fig. 4) is that of a rarefaction wave type or deflagration type. A neutral gas with velocity u_1 and density ρ_1 enters the discharge layer and becomes ionized, leaving the current layer with velocity u_2, which can be calculated approximately from the conservation of momentum (because of the assumption of stationary process $d/d\tau = 0$, $V_p = V_f = 0$):

$$\rho_1 u_1 u_2 = (B_1^2/2\mu) \quad (9)$$

where $(B_1^2/2\mu)$ represents the magnetic pressure at section 1. Because the gas at section 1 is not ionized, magnetic pressure (more exactly, Lorentz force) is directed downstream.

From conservation of mass ($\rho_1 u_1 = \rho_2 u_2$), it follows that because $u_1 \ll u_2$

$$(\rho_2/\rho_1) \ll 1 \quad (10)$$

Therefore, the acceleration in this device is indeed associated with the decrease of density (rarefaction-like process). It is known from basic gasdynamics that such a process is efficient.

Simplified model of a discharge layer

We shall assume that at section 1 there is a preheating zone where temperature rises up to the ionization temperature with relatively small current density j. Acceleration of the gas in this region occurs due to Joule heating. It is known from gasdynamics that the maximum speed obtained in the steady flow with heat addition to the gas is a sonic speed. Assuming the thermodynamic equilibrium this speed is given by the relation

$$u_i = (\gamma R T_{\text{ion}})^{1/2} \quad (11)$$

where $R = km = c_p - c_v$ is the gas const and T_i is the ionization temperature.

If one assumes that, starting from this section main acceleration mechanism is that of $\mathbf{j} \times \mathbf{B}$ force, one obtains from conservation of momentum

$$(B_1^2/2\mu) = \rho_1 u_1(u_2 - u_i) - p_i + p_2 \quad (12)$$

Taking into account that, because the current sheet is stationary, $\partial B/\partial\tau = 0$, the electric field according to Maxwell equation must be constant across the sheet. From Ohm's law, it follows that

$$E = Bu - (1/\sigma\mu)(\partial B/\partial\xi) \quad (13)$$

where σ is electric conductivity and μ is permeability.

Assuming very high conductivity at section i, one obtains

$$\frac{B_1^2 u_i}{\mu} = \rho_1 u_1 \left(\frac{u_2^2}{2} - \frac{u_i^2}{2}\right) - \rho_1 u_1 (c_p T_i - c_p T_2) \quad (14)$$

From Eq. (13) it follows that, because at section 2 $B_2 = 0$ conductivity, σ_2 must be also zero (low temperature). Therefore one can neglect $c_p T_2$ and p_2.

From Eq. (14) and conservation of mass ($\rho_1 u_1 = \rho_i u_i$), one obtains

$$(u_2^2/2) - (u_i^2/2) - c_p T_i = 2u_i(u_2 - u_i) - 2(p_i/\rho_i)$$

or

$$[(p_i/\rho_i) = (c_p - c_v)T_i]$$

$$(u_2^2/2) - 2u_i u_2 + \tfrac{3}{2} u_i^2 - (2c_v - c_p)T_i = 0$$

therefore

$$u_2 = 2u_i \pm [u_i^2 + 2(2c_v - c_p)T_i]^{1/2} = u_i\left[2 \pm \left(1 + \frac{2(2-\gamma)}{\gamma(\gamma-1)}\right)^{1/2}\right] \quad (15)$$

For $\gamma = \frac{5}{3}$ ($u_2 > u_i$), $u_2 = 3.27\ u_i$. For hydrogen $T_i = 15000°\text{K}$, $u_i \cong 15000$ m/sec. Therefore, $u_2 = 4.9 \times 10^6$ cm/sec. The order of magnitude of this velocity is in agreement with experimentally observed values.

Calculation of mass flow

From the momentum equation applied to sections 1 and i (Fig. 4), it follows that

$$p_1 + \rho_1 u_1^2 = p_i + \rho_i u_i^2$$

or

$$\frac{p_1}{\rho_1 u_1} + u_1 = \frac{p_i}{\rho_i u_i} + u_i$$

Taking into account that

$$(p/\rho) = RT \text{ and } u_i = (\gamma R T_i)^{1/2}$$

one obtains

$$\frac{R_1 T_1}{u_1} + u_1 = \left(\frac{R_i T_i}{\gamma}\right)^{1/2} + (\gamma R_i T_i)^{1/2} = \frac{\gamma+1}{\gamma}(\gamma R_i T_i)^{1/2}$$

or

$$u_1 = \frac{1}{2}\left[\frac{\gamma+1}{\gamma}[\gamma R_i T_i]^{1/2} \pm \left(\frac{(\gamma+1)^{1/2}}{\gamma} R_i T_i - 4R_1 T_1\right)^{1/2}\right] \quad (16)$$

Taking into account that $R_1 T_1 \ll R_i T_i$, $u_1 < u_i$, and assuming that $R_1 = R_i$, one can develop expression (16) obtaining

$$u_1 \cong \frac{R_1 T_1 \gamma^{1/2}}{(\gamma+1) R_i T_i}$$

or

$$\rho_1 u_1 = \frac{p_1 \gamma^{12}}{(\gamma+1)(R_i T_i)^{1/2}} \quad (17)$$

u_1 is the velocity of the gas in the system of coordinates connected with the sheet $u_1 = v_1 - U$. If the gas velocity is slightly different than u_1 ($v_1 \neq u_1$), the sheet must move with the velocity $U = v_1 - u_1$; for $v_1 < u_1$, the sheet moves toward insulator $U < 0$; and for $v_1 > u_1$, the sheet moves toward the exit $U > 0$.

In this simplified model of stationary current sheet, the ionization current has been neglected. However, ionization current can be quite important, and the detailed analysis of the structure of the discharge layer is necessary for better understanding the acceleration process.

There is, of course, the possibility of utilizing the principle of "deflagration" type of current layer in a pulsed gas device.‡ Such a system will combine the advantage of the gasdynamic cycle of an arcjet with the mean low-power requirement of a pulse device. Moreover, the nonsteady flow enables one to obtain higher mass flow [$V_{max} = 2a_0/(\gamma - 1)$, where a_0 is the reservoir sound speed] than that of steady flow {where $V_{max} = [2/(\gamma-1)^{1/2} a_0]$}.

Conclusions

1) The current layer sweeping up the gas leads to significant losses.

2) The velocity distribution characteristic for an expanding layer leads to smaller losses.

3) Deflagration type of stationary discharge layer is in principle very efficient and can provide high specific impulse.

References

[1] Samaras, D. G., *Applications of Ion Flow Dynamics* (Prentice-Hall, Inc., Englewood Cliffs, N. J., 1962), p. 417.

[2] Stuhlinger, E., "Electric propulsion," Astronautics and Aeronautics **1**, 26 (1964).

[3] Rosciszewski, J., "Preliminary study of the ionizing front in a plasma gun," General Dynamics/Astronautics, Space Science Lab. Rept. BBI-63-003 (March 1963).

[4] Goldstein, S., *Lectures on Fluid Mechanics* (Interscience Publishers, Inc., New York, 1960), p. 59.

‡ Recently Gooding and Ashley of General Dynamics/Astronautics obtained experimentally such a stationary layer in a pulse device.

Thermorheologically Simple Viscoelastic Materials

M. Shinozuka*

Columbia University, New York, N. Y.

WITHIN the framework of linear theory, the thermal stress analysis of homogeneous, isotropic, thermorheologically simple viscoelastic materials has been developed by Morland and Lee[1] and Muki and Sternberg.[2] This analysis is based on the temperature-time equivalence hypothesis with reference to the relaxation modulus

$$G_{T_1}(t) = G_{T_0}[\varphi(T_1)t] \quad (1)$$

where t denotes the time, $G_T(t)$ the relaxation modulus of the material at temperature T, T_0 the base temperature, and $\varphi(T_1)$ is the shift factor at $T = T_1$. The shift factor satisfies $\varphi(T) > 0$, $\varphi(T_0) = 1$, and $d\varphi(T)/dT > 0$.

The purpose of this note is to show explicitly how the temperature-time equivalence hypothesis can be formulated in terms of the temperature dependence of the relaxation spectrum of the material, since relaxation spectra among the various viscoelastic functions are most closely related to the molecular processes occurring in the material, and since hypothesis stated with respect to spectra is expected to indicate more clearly the validity and limitations of stress-strain relations of thermorheologically simple materials.

Under zero initial conditions and uniform temperature T, the deviatoric stress-strain relations are

$$s_{ij}(x,t) = \int_0^t G_T(t-t')\dot{e}_{ij}(x,t')dt' \text{ or } e_{ij}(x,t) = \int_0^t J_T(t-t')\dot{s}_{ij}(x,t')dt' \quad (2)$$

Received September 2, 1964. This work was supported by the Office of Naval Research under contract Nonr 266(78).

* Assistant Professor of Civil Engineering.